Development and Understanding of High-Performance Solid Oxide Electrolysis Cells

PI: Xiao-Dong Zhou

Stuller Endowed Chair in Chemical Engineering
Institute for Materials Research and Innovation
University of Louisiana at Lafayette
Lafayette, LA 70503
Email: zhou@louisiana.edu

PM: Evelyn Lopez

Jason Montgomery (2021)

9:30 am on October 27, 2022; DE-FE0032110

Technical Questions Addressed

1. What is the origin for the electrochemically driven phase change in an SOC electrode?
   What would be the theoretical model based on measurable variables to predict this phenomenon?
   How to validate the theoretical understanding?

PNAS RESEARCH ARTICLE | ENGINEERING

Origin for electrochemically driven phase transformation in the oxygen electrode for a solid oxide cell

Emir Dogdibegovic[a], Yudong Wang[a,b,1], and Xiao-Dong Zhou[a,b,1]

Edited by Alexis Bell, University of California, Berkeley, CA; received February 28, 2022; accepted September 16, 2022

https://www.pnas.org/doi/10.1073/pnas.2203256119

2. Why is the performance stable while the nickelates go through a severe phase transition?
   What is the thermodynamic base for conjugated phenomenon between activity and stability?
   How does the interface influence the activity/durability relationship?

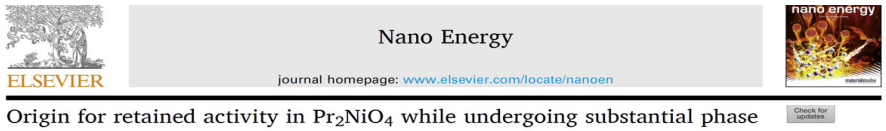

ELSEVIER

Nano Energy

journal homepage: www.elsevier.com/locate/nanoen

Origin for retained activity in Pr_2NiO_4 while undergoing substantial phase transformation in a long-term solid oxide cell operation

Emir Dogdibegovic [a], Yudong Wang [a,b], Christopher J. Wright [a], Xiao-Dong Zhou [a,b,*]

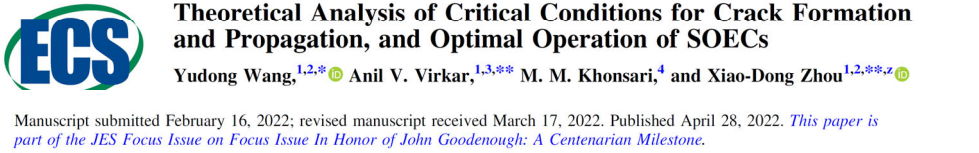

Journal of The Electrochemical Society, 2022 **169** 044529

Theoretical Analysis of Critical Conditions for Crack Formation and Propagation, and Optimal Operation of SOECs

Yudong Wang,[1,2,*] Anil V. Virkar,[1,3,**] M. M. Khonsari,[4] and Xiao-Dong Zhou[1,2,**,z]

Manuscript submitted February 16, 2022; revised manuscript received March 17, 2022. Published April 28, 2022. *This paper is part of the JES Focus Issue on Focus Issue In Honor of John Goodenough: A Centenarian Milestone.*

3. How to use the understanding of electrochemically driven phase change to develop reliable and reproducible accelerated measurements?
   What is the physical process being accelerated?
   What are accelerated test protocols for other constituents and electrochemical systems?

Technical Questions to Be Addressed

Cost (1$/kg-$H_2$):
How to achieve high-performance SOECs?

Durability (A/1000-h or W/1000-h)
What are the factors limiting the performance stability of an SOEC?

Technical questions to be addressed by this project

- **How to establish theoretical understanding of the durability of SOECs based on measurable variables?**
- **What are the effects of operating modes (e.g., constant *I* and constant *V*) and materials properties on the SOEC performance durability?**
- **How to calculate crack growth rate with respect to measurable properties?**
- **What are the factors limiting cell current density and durability?**
- **Is delamination inevitable? Is there a critical condition for the delamination?**
- **How does the interlayer chemistry at the oxygen electrode side influence current density and performance durability? How about the fuel electrode?**
- **What's the proper accelerated test method to study SOECs?**

Team Members

Program Managers:
Dr. Evelyn Lopez, 3610 Collins Ferry Road, Morgantown, WV 26507

Personnel at University of Louisiana at Lafayette

Xiao-Dong Zhou	Principal Investigator
Henry Chu	Co-PI and Informatics Center Director
Tom Pesacreta	Co-PI and Microscope Center Director
Yudong Wang	Co-Investigator
Atif Niaz	Postdoc Researcher
Keying Xu	Postdoc Researcher
Christabel Adjah-Tetteh	Graduate student
Scott Blazer	Graduate student
Austin Schilling	Undergraduate student

Solid Oxide Cells: Coupled O^{2-}/e^- Transport
SOFC to generate electricity; SOEC to produce H_2

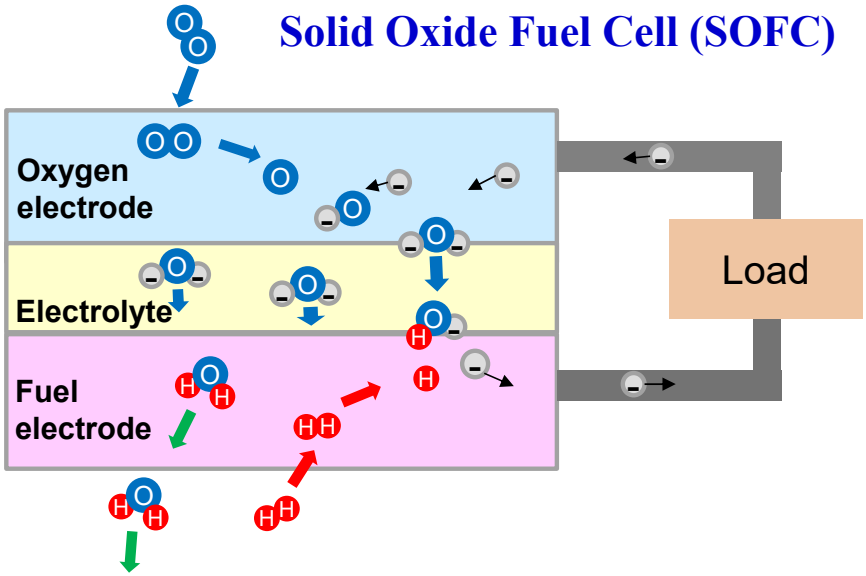

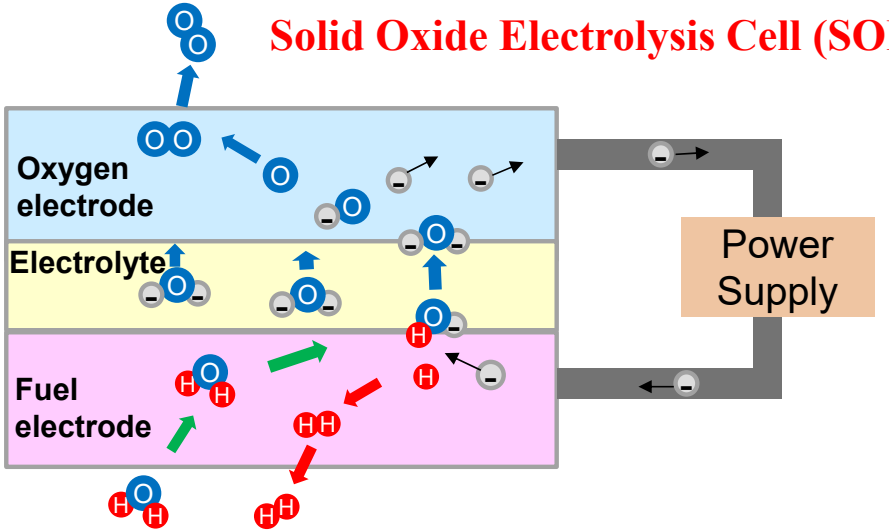

Oxygen Electrode: $\frac{1}{2}O_2 + 2e^- \rightarrow O^{2-}$

Electrolyte: High O^{2-} conductivity. Low e^- conductivity.

Fuel Electrode: $H_2 + O^{2-} \rightarrow H_2O + 2e^-$

Oxygen Electrode: $O^{2-} \rightarrow \frac{1}{2}O_2 + 2e^-$

Electrolyte: High O^{2-} conductivity. Low e^- conductivity.

Fuel Electrode: $H_2O + 2e^- \rightarrow H_2 + O^{2-}$

Analysis of μ_{O_2} Distribution in Solid Oxide Cells

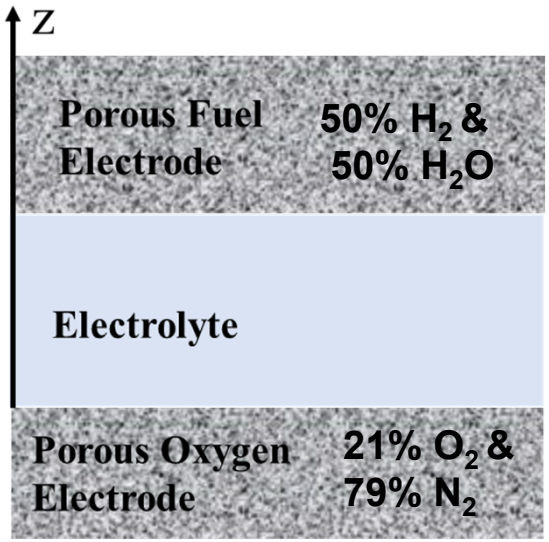

- Local chemical equilibrium occurs at $\vec{r}$ in the solid electrolyte.

$$O_2(\vec{r}) + 4e^-(\vec{r}) \rightleftharpoons 2O^{2-}(\vec{r})$$

$$\mu_{O_2}(\vec{r}) = 2\,\tilde{\mu}_{O^{2-}}(\vec{r}) + 4F\varphi(\vec{r})$$

- Two independent fluxes are ionic current and electronic current

$$I_i = \frac{\sigma_i}{2F}\frac{d}{dz}\tilde{\mu}_{O^{2-}}$$

$$I_e = -\sigma_e \frac{d}{dz}\varphi$$

- Governing equations (steady state):

Oxygen conservation: $\frac{d}{dz} I_i = 0$

Charge conservation: $\frac{d}{dz}(I_i + I_e) = 0$

Boundary	Equation
Electrolyte/Fuel electrode ($z = l$)	$I_e = -\frac{1}{r_e^{FE}}(\varphi^{FE} - \varphi^{el})$
	$I_i = \frac{1}{4Fr_i^{FE}}(\mu_{O_2}^{FE} - 4F\varphi^{FE} - \mu_{O_2}^{el} + 4F\varphi^{el})$
Electrolyte / Oxygen electrode ($z = 0$)	$I_e = \frac{1}{r_e^{OE}}(\varphi^{OE} - \varphi^{el})$
	$I_i = -\frac{1}{4Fr_i^{OE}}(\mu_{O_2}^{OE} - 4F\varphi^{OE} - \mu_{O_2}^{el} + 4F\varphi^{el})$

Wang. Y. et al. *Journal of The Electrochemical Society, (*2022) 169 044529
Virkar, A. V. *Journal of Power Sources* 147.1-2 (2005): 8-31

Effect of Operating Voltage on μ_{O_2} Distribution in the Electrolyte of Solid Oxide Cells

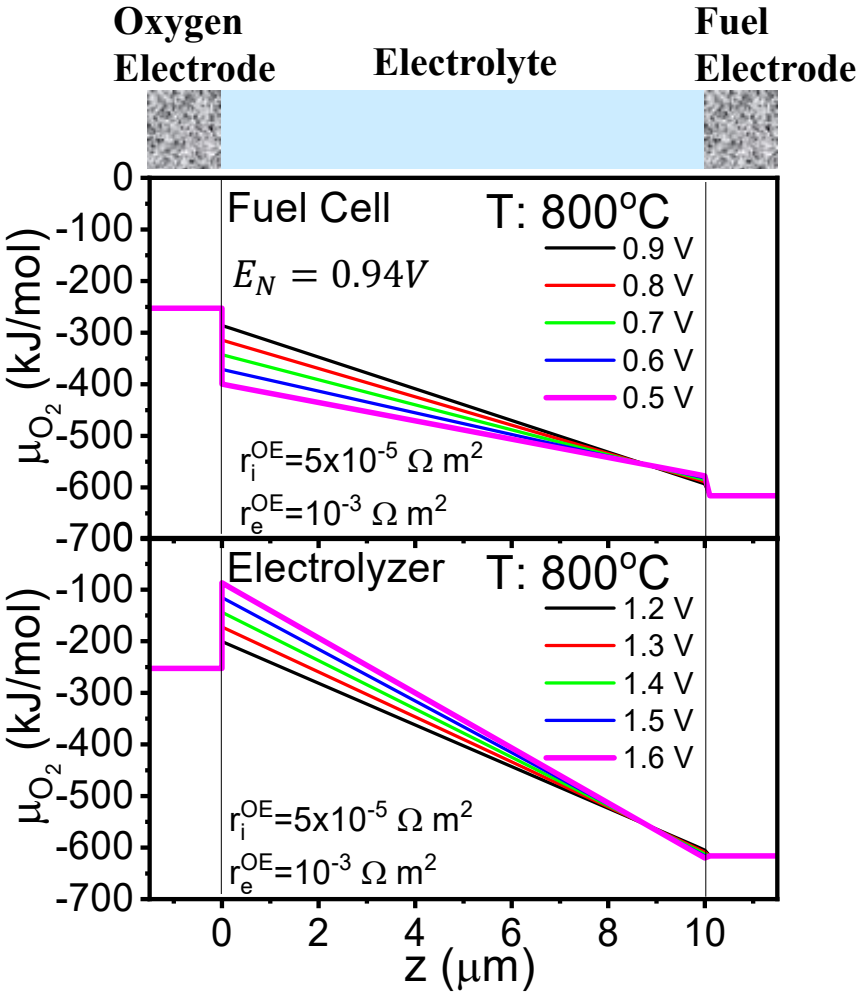

- Nernst voltage: $E_N = \frac{\mu_{O_2}^{OE} - \mu_{O_2}^{FE}}{4F}$
- $V_{cell} < E_N$ Discharging, fuel cell mode
- $V_{cell} > E_N$ Charging, electrolyzer mode

$$\mu_{O_2}^{OE|El} = \mu_{O_2}^{OE} + 4F(\boldsymbol{V_{cell}} - E_N)\frac{r_i^{OE}}{R_{i,t}} - 4F\boldsymbol{V_{cell}}\frac{r_e^{OE}}{R_{e,t}}$$

$$p_{O_2} = p_0 \exp\left(\frac{\mu_{O_2} - \mu_{O_2}^0}{RT}\right)$$

The p_{O_2} Distribution in the Electrolyte of Solid Oxide Cells

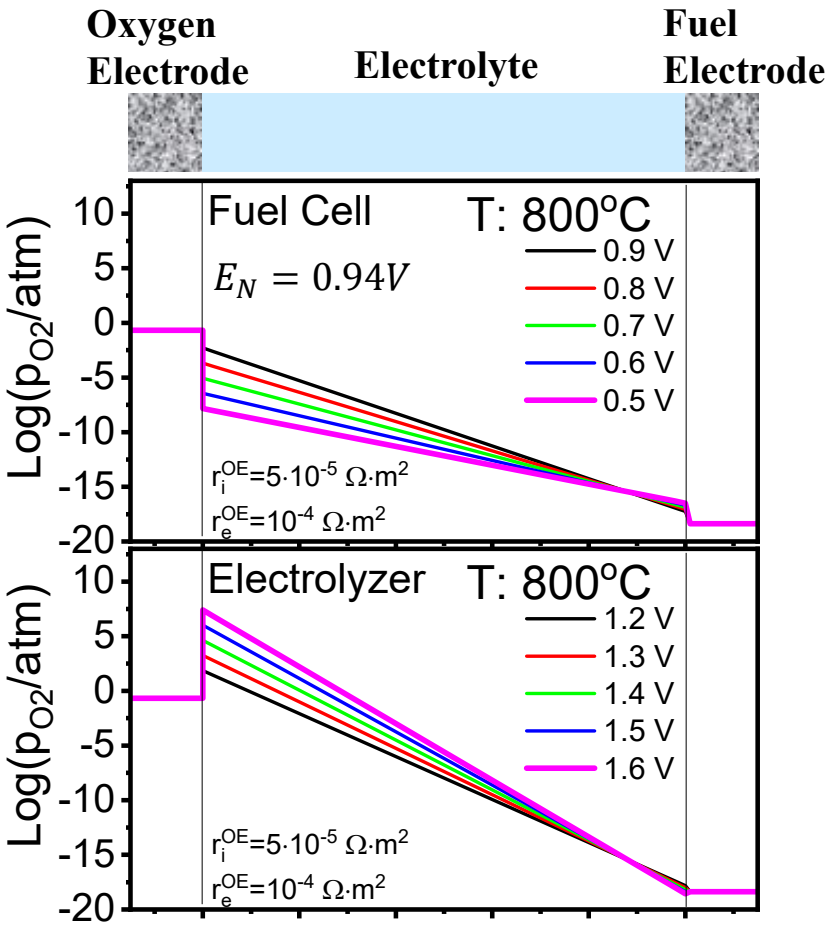

- Nernst potential: $E_N = \frac{\mu_{O_2}^{OE} - \mu_{O_2}^{FE}}{4F}$
- $V_{cell} < E_N$ Discharging, fuel cell mode
- $V_{cell} > E_N$ Charging, electrolyzer mode

$$\mu_{O_2}^{OE|El} = \mu_{O_2}^{OE} + 4F(V_{cell} - E_N)\frac{r_i^{OE}}{R_{i,t}} - 4FV_{cell}\frac{r_e^{OE}}{R_{e,t}}$$

$$p_{O_2} = p_0 \exp\left(\frac{\mu_{O_2} - \mu_{O_2}^0}{RT}\right)$$

- Under fuel cell mode, p_{O_2}<0.21atm, OE|EL is under reducing condition

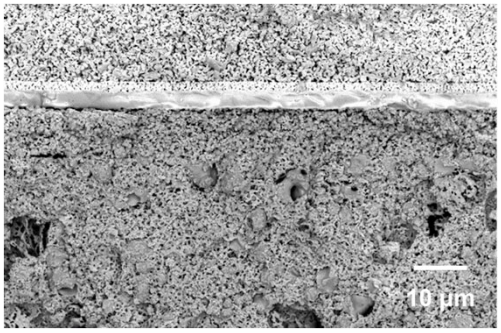

- Under electrolyzer mode, p_{O_2} can induce high pressure (42,477 atm @1.4V)

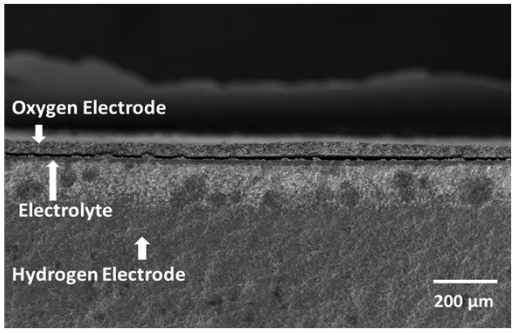

Analysis on Electrochemically Driven Phenomenon

Hence, during cell operation, μ_{O_2} within the electrolyte is mathematically bounded by corresponding values at the two electrodes (gas phases), meaning $\mu_{O_2}^{cathode} \geq \mu_{O_2}^{c} > \mu_{O_2}^{a} \geq \mu_{O_2}^{anode}$ which can be derived as follows:

$$\mu_{O_2}^{c} = \mu_{O_2}^{cathode} + 4e(r_i^c I_i - r_e^c I_e) = \mu_{O_2}^{cathode} - 4e(r_i^c |I_i| + r_e^c |I_e|) < \mu_{O_2}^{cathode}$$

Reducing condition in the interfaces. Assuming the ideal gas law for oxygen, we obtain $\boldsymbol{\mu_{O_2}^{cathode} = \mu_{O_2}^{o} + k_B T ln(P_{O_2}^{cathode})}$, where $\mu_{O_2}^{o}$ is standard state gas phase oxygen chemical potential and $P_{O_2}^{cathode}$ is the oxygen partial pressure at the cathode (gas phase). Eq. [5] gives:

$$P_{O_2}^{c} \approx P_{O_2}^{cathode} \exp[-\frac{\boldsymbol{4e(r_i^c |I_i| + r_e^c |I_e|)}}{k_B T}]$$

- $P_{O_2}^{c} < P_{O_2}^{cathode}$.
- $P_{O_2}^{c} / P_{O_2}^{cathode} \sim (r_i^c |I_i| + r_e^c |I_e|)$.
- T = 800°C (1073 K), $\boldsymbol{(r_i^c |I_i| + r_e^c |I_e|) = 0.2}$ **V**; $P_{O_2}^{cathode}$ = 0.21 atm; then $\boldsymbol{P_{O_2}^{c} \approx 3.7 \times 10^{-5}}$ **atm**.
- The local oxygen partial pressure (the level of reducing condition) depends on both $r_i^c |I_i|$ and $\boldsymbol{r_e^c |I_e|}$. The most reducing location is at the immediate cathode/electrolyte interface.

Overpotential	0.05 V	0.1 V	0.2 V	0.3 V	0.4 V
$P_{O_2}^{c}$ **(atm)**	0.024	0.0029	3.7×10^{-5}	4.9×10^{-7}	6.5×10^{-9}

A. V. Virkar, *Journal of Power Sources,* 172[2] 713-24 (2007).
Dogdibegovic, Wang, and Zhou, PNAS (2022)

Thermal vs. Electrochemical Phase Evolution

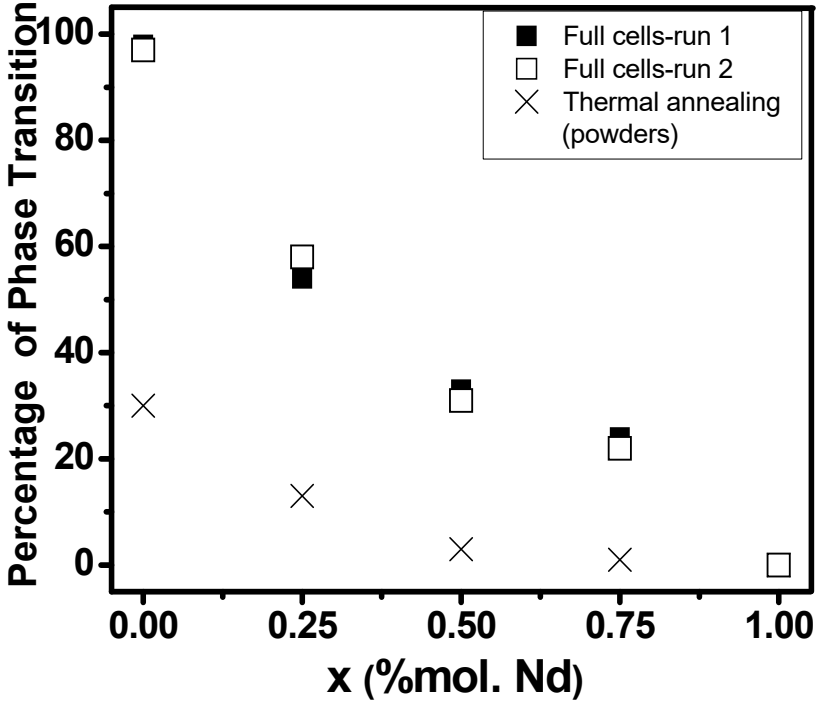

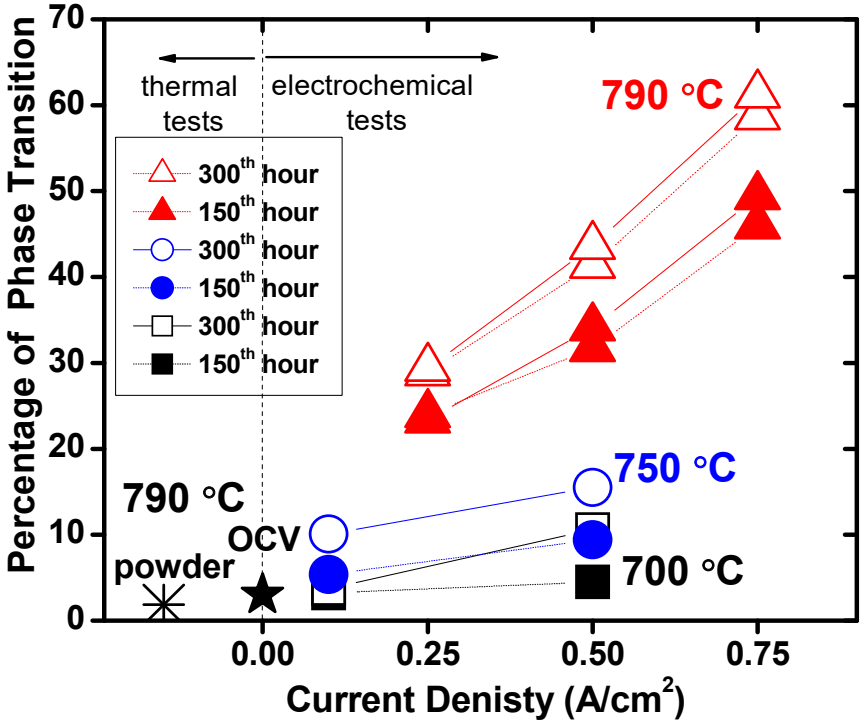

Points to take

- **Reproducible** results with multiple cells per each condition.
- Phase evolution is **accelerated** with electrochem. operation in full cells.
- Relatively stable cathode materials (in thermal equilibrium) may not be stable in SOFCs.

Dogdibegovic, Wang, and Zhou, PNAS, 2022

Performance Stability vs. Interlayer Chemistry

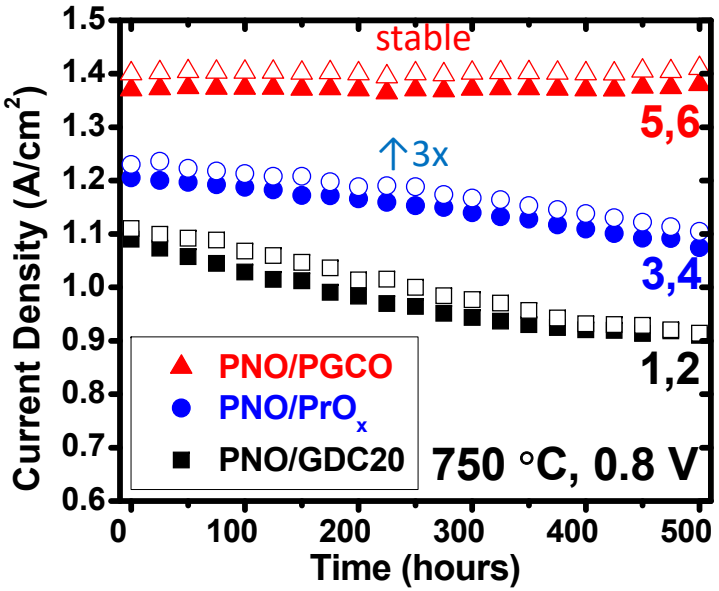

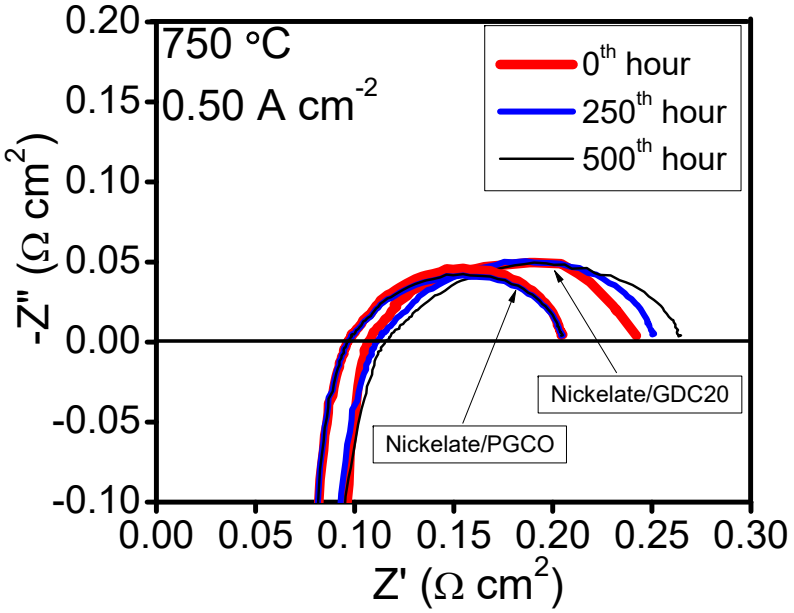

Points to take:

- Multiple cells for each condition for both PNO and PNNO electrodes
- 3x reduced performance degradation in PNO/PrO$_x$ cells.
- Stable operation was measured on multiple sets of cells and cathode compositions with the PGCO interlayer.
- Reduced R_{pol} (↑MIEC → ↑σ_e) due to extended rxn. zone.
- Reduced Rohm (↓Rgb with [Pr]↑)[1]

Summarized ASR vs. GDC cells.

ASR	Ohmic	Electrode	Total
PrOx-GDC 500th hour	7%↓	22%↓	15%↓
PGCO 500th hour	16%↓	28%↓	22%↓

[1]S. Lübke et al. *SSI*, **117**, p.229 (1999).

Distribution of μ_{O_2} in an Electrolysis Cell

Absence of crack formation

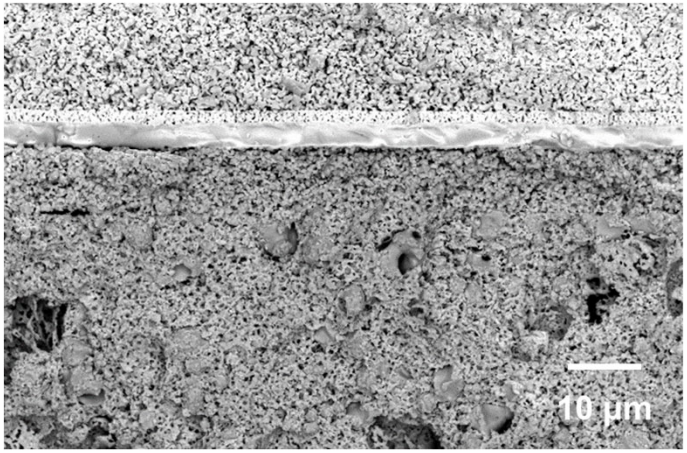

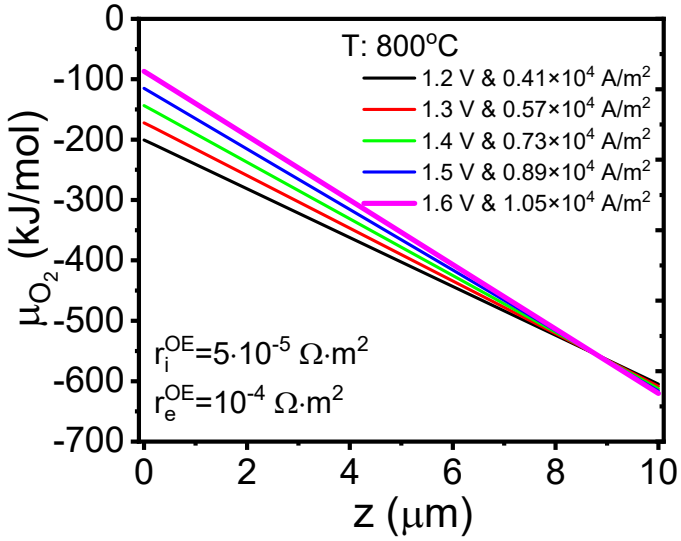

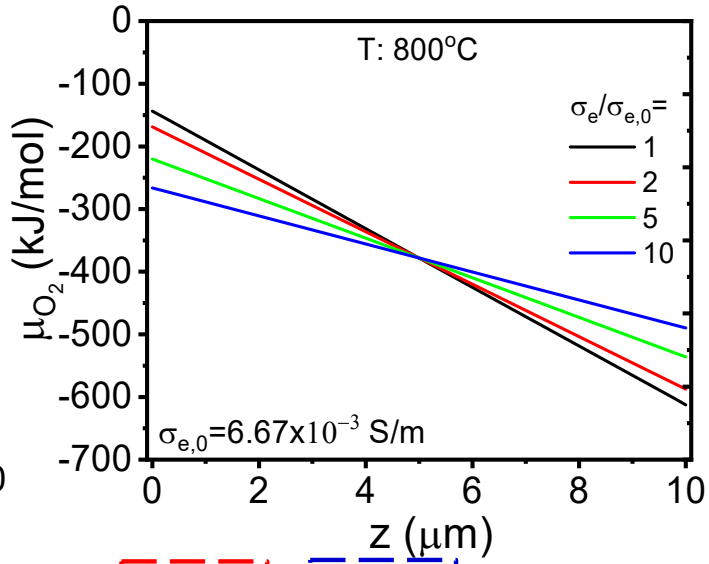

Analytical result:

$$\mu_{O_2}(z) = \mu_{O_2}^{OE} + 4FI_i\left(r_i^{OE} + \frac{z}{\sigma_i}\right) - 4FI_e\left(r_e^{OE} + \frac{z}{\sigma_e}\right)$$

Ionic flux contribution

electronic flux contribution

$$\mu_{O_2}^{OE|El} = \mu_{O_2}^{OE} + 4FI_i r_i^{OE} + 4FI_e r_e^{OE}$$

- High operation voltage/current raises μ_{O_2} at OE|EL (z=0) in most cases.
- Raising σ_e decreases μ_{O_2} at OE|EL (z=0) and reduces Faradaic efficiency

$$I_i = \frac{V_{cell} - E_N}{R_{i,t}}$$

$$I_e = \frac{V_{cell}}{R_{e,t}}$$

Wang. Y. et al. *Journal of The Electrochemical Society, 2022 169 044529*

Analysis of μ_{O_2} Distribution in Solid Oxide Cells

Effect of transport properties, constant V and constant I

Analytical result at OE:

$$\mu_{O_2}^{OE|El} = \mu_{O_2}^{OE} + 4F(V_{cell} - E_N)\frac{r_i^{OE}}{R_{i,t}} - 4FV_{cell}\frac{r_e^{OE}}{R_{e,t}}$$

$$\mu_{O_2}^{OE|El} = \mu_{O_2}^{OE} + 4FI_i r_i^{OE} + 4F(E_N - R_{i,t}I_i)\frac{r_e^{OE}}{R_{e,t}}$$

- Constant V_{cell} : $\downarrow r_i^{OE}$, $\downarrow \mu_{O_2}^{OE|El}$ operation reaches a maximum $\mu_{O_2}^{OE|El}$; Constant I_i operation has linear $\mu_{O_2}^{OE|El}$-r_i^{OE} relation.
- Constant I_i operation is only suitable for stable oxygen electrodes.
- $\uparrow r_e^{OE}$ significantly $\downarrow \mu_{O_2}^{OE|El}$

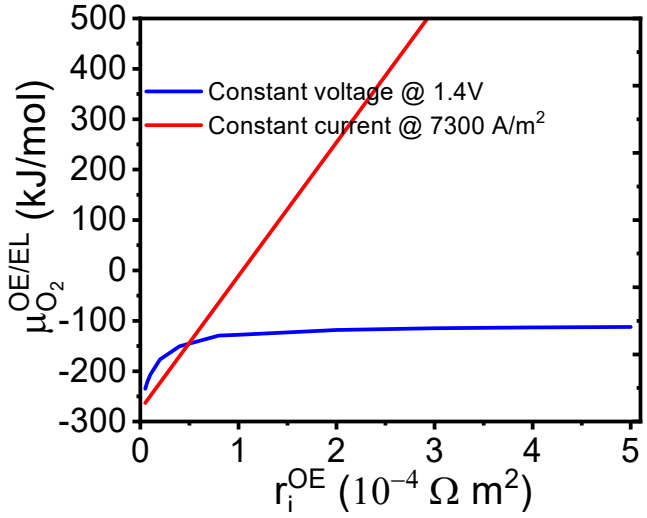

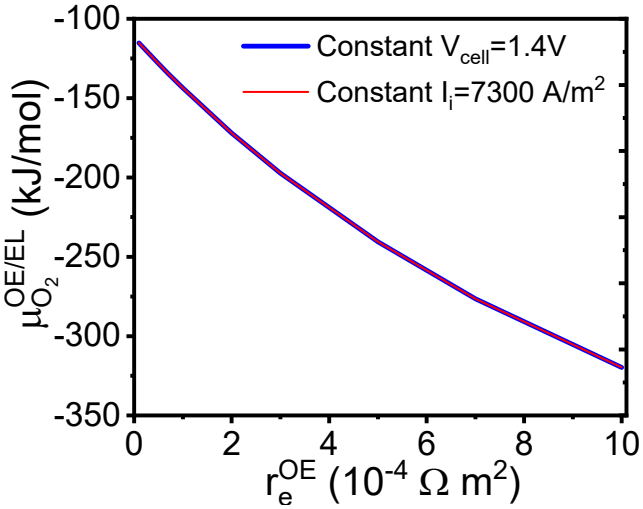

$$\left(\frac{\partial \mu_{O_2}^{OE|El}}{\partial r_i^{OE}}\right)_{V_{cell}} = 4F\frac{V_{cell} - E_N}{R_{i,t}}\left(\frac{R_{i,t} - r_i^{OE}}{R_{i,t}}\right) \qquad \left(\frac{\partial \mu_{O_2}^{OE|El}}{\partial r_e^{OE}}\right)_{V_{cell}} = 4FV_{cell}\left(\frac{R_{e,t} - r_e^{OE}}{R_{e,t}^2}\right)$$

$$\left(\frac{\partial \mu_{O_2}^{OE|El}}{\partial r_i^{OE}}\right)_{I_i} = 4FI_i\left(\frac{R_{e,t} - r_e^{OE}}{R_{e,t}}\right) \qquad \left(\frac{\partial \mu_{O_2}^{OE|El}}{\partial r_e^{OE}}\right)_{I_i} = 4F(E_N - R_{i,t}I_i)\left(\frac{R_{e,t} - r_e^{OE}}{R_{e,t}^2}\right)$$

Analysis of μ_{O_2} Distribution in Solid Oxide Cells

Effect of electrolyte thickness and fuel composition

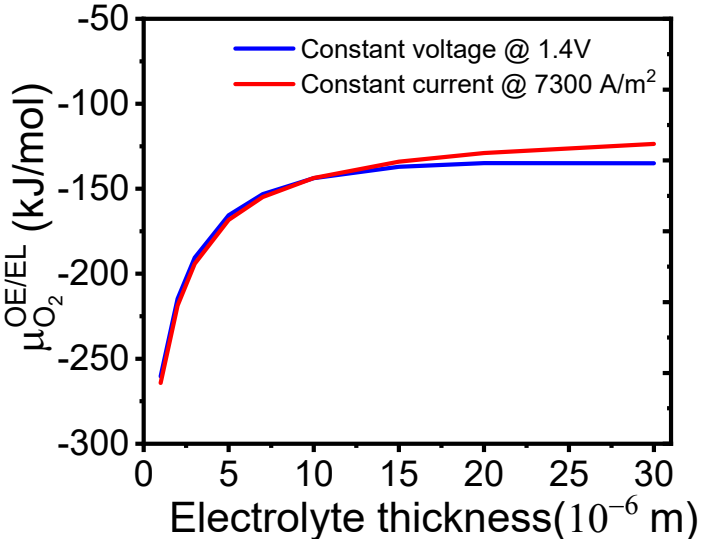

$$\left(\frac{\partial \mu_{O_2}^{OE|El}}{\partial l}\right)_{V_{cell}} = -4F(V_{cell} - E_N)\frac{r_i^{OE}}{\sigma_i R_{i,t}^2} + 4FV_{cell}\frac{r_e^{OE}}{\sigma_e R_{e,t}^2}$$

$$\left(\frac{\partial \mu_{O_2}^{OE|El}}{\partial l}\right)_{I_i} = -4\mathrm{F}I_i\frac{r_e^{OE}}{\sigma_i R_{e,t}} + 4FR_{i,t}I_i\frac{r_e^{OE}}{\sigma_e R_{e,t}^2}$$

- ↓ **electrolyte thickness** (l), ↓ $\boldsymbol{\mu_{O_2}^{OE|El}}$.

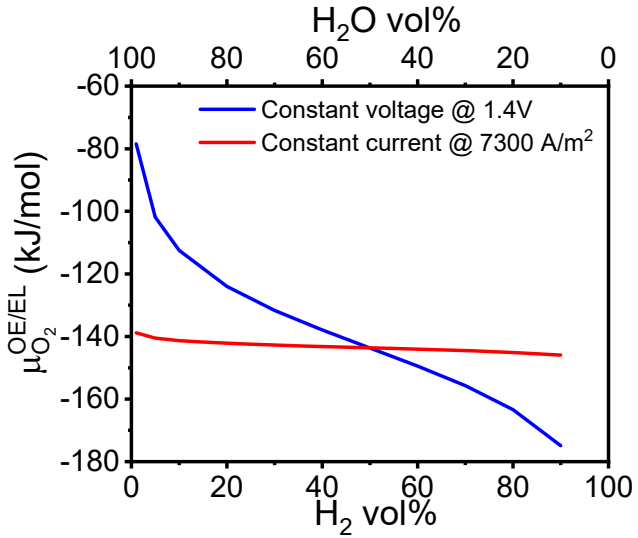

$$\left(\frac{\partial \mu_{O_2}^{OE|El}}{\partial x_{H_2}^{FE}}\right)_{V_{cell}} = -\frac{\mathrm{RT}}{x_{H_2}^{FE}(1-x_{H_2}^{FE})}\frac{\boldsymbol{r_i^{OE}}}{\boldsymbol{R_{i,t}}}$$

$$\left(\frac{\partial \mu_{O_2}^{OE|El}}{\partial x_{H_2}^{FE}}\right)_{I_i} = -\frac{\mathrm{RT}}{x_{H_2}^{FE}(1-x_{H_2}^{FE})}\frac{\boldsymbol{r_e^{OE}}}{\boldsymbol{R_{e,t}}}$$

- ↑ H_2 vol% can significantly ↓ $\mu_{O_2}^{OE|El}$ (**constant V**)
- $\boldsymbol{\mu_{O_2}^{OE|El}}$ **is stable** with change H_2 vol% (**constant I**)

Wang. Y. et al. *Journal of The Electrochemical Society, 2022 169 044529*

$p_{O_2}^{TPB}$: Transport Property Effect

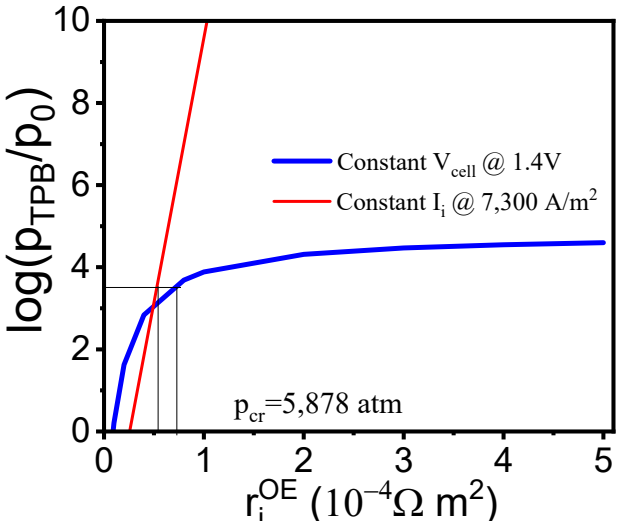

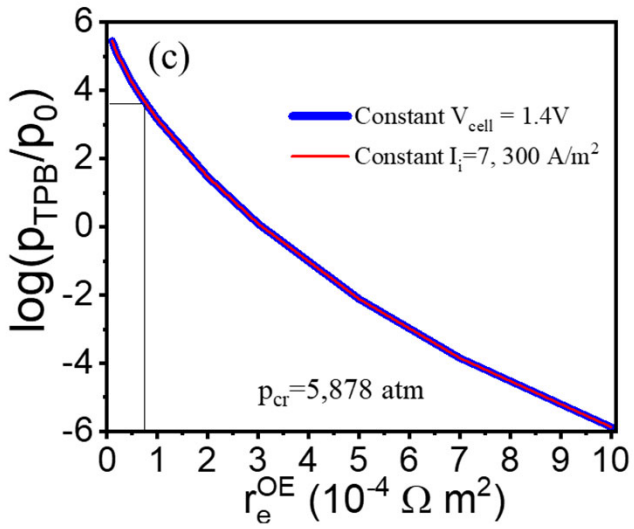

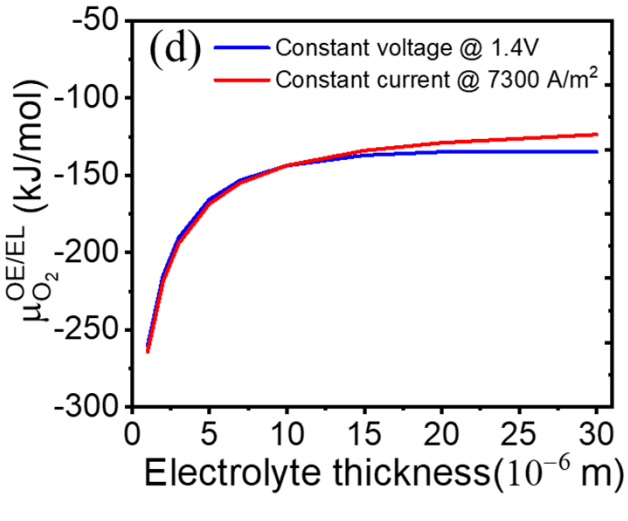

- $p_{cr} = 5{,}878$ atm with crack radius of 1 μm
- A low r_i^{OE} is preferred to suppress $p_{O_2}^{TPB}$. At a constant V_{cell} of 1.4 V, the critical r_i^{OE} is ~ 5.4×10^{-5} Ω m². For a constant I_i of 7,300 A/m², the critical r_i^{OE} is 7.5×10^{-5} Ω m².
- A constant current electrolysis is not suitable for studying an unstable electrode material, which potentially leads to the formation of cracks and even electrode delamination.
- A high r_e^{OE} is in favor of reducing $p_{O_2}^{TPB}$.

Wang. Y. et al. *Journal of The Electrochemical Society* (2022)

$p_{O_2}^{TPB}$: Operation Condition Effect

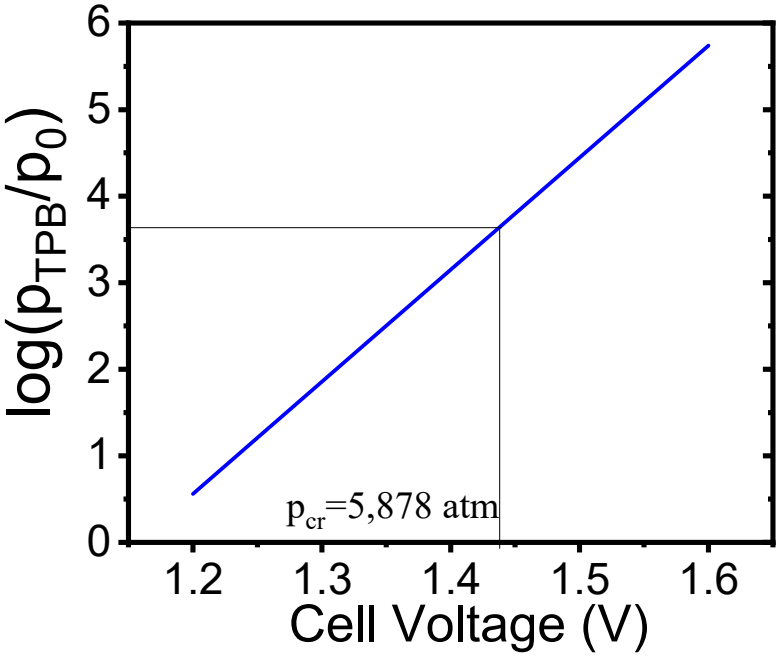

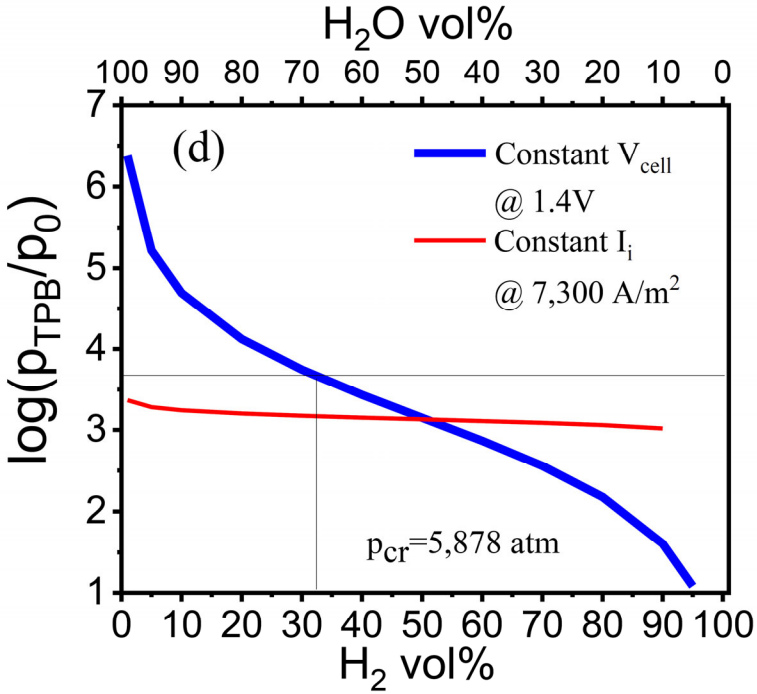

- V_{cell} is higher than 1.44 V leads to $p_{O_2}^{TPB} > p_{cr}$ under the simulated conditions
- A low H_2 vol% in the fuel electrode results in a high $p_{O_2}^{TPB}$ at constant voltage operation and a concentration less than 32% can lead to crack growth.
- The effect of H_2 vol% on $p_{O_2}^{TPB}$ is marginal under a constant current electrolysis.

Wang. Y. et al. *Journal of The Electrochemical Society* (2022)

SOEC with a Penny-shaped Crack
Criterion for Griffith Crack to Propagate

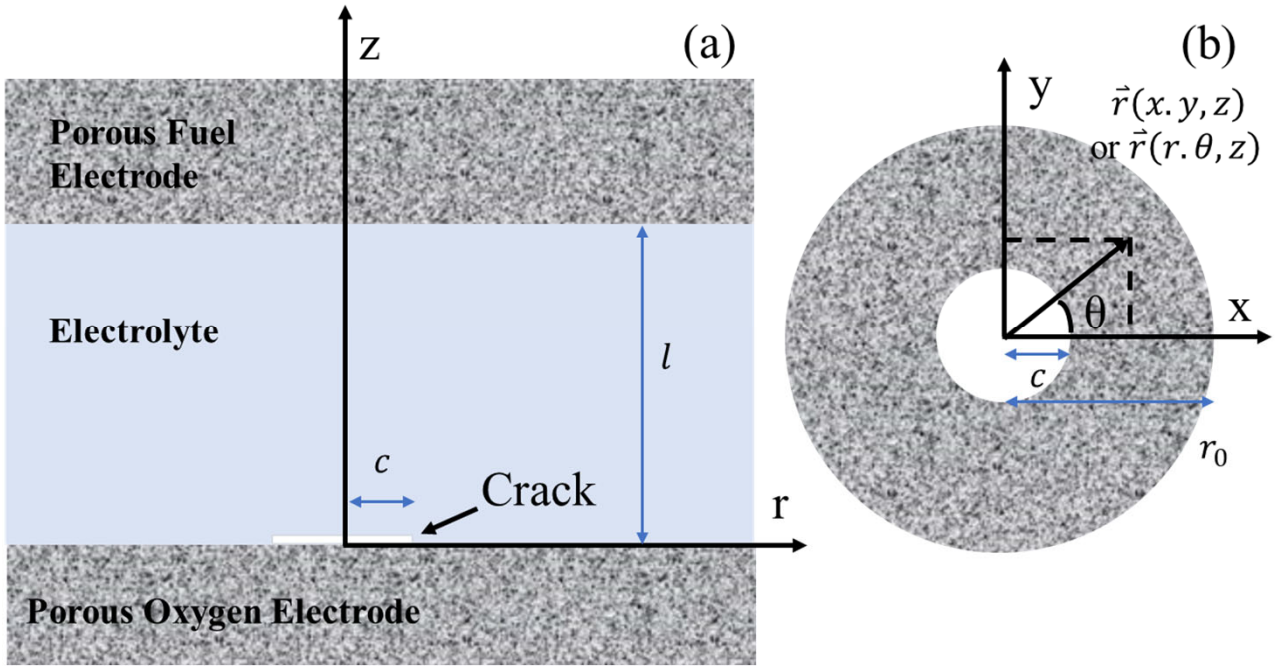

- The crack can not conduct $\boldsymbol{I_i}$ or $\boldsymbol{I_e}$. On the surface of crack

$$\boldsymbol{I_i} \cdot \boldsymbol{n_{crack}} = 0 \quad \boldsymbol{I_e} \cdot \boldsymbol{n_{crack}} = 0$$

- At the edge of the crack (r=c) is TPB

$$\frac{1}{2}O_2(crack) + 2e^-(OE) \rightleftharpoons O^{2-}(SE)$$

- $\Delta G_m < 0 \Leftrightarrow \mu_{O_2}^{Crack} > \mu_{O_2}^{TPB}$: Oxygen moves out from the crack
- $\Delta G_m > 0 \Leftrightarrow \mu_{O_2}^{Crack} < \mu_{O_2}^{TPB}$: Oxygen pumped into the crack

$$p_{O_2}^{TPB} = p_0 \exp\left(\frac{\mu_{O_2}^{TPB} - \mu_{O_2,T}^0}{RT}\right)$$

$$p_{cr} = \sqrt{\frac{\pi \gamma_{eff} E}{2(1-\nu^2)c}}$$

- The existing crack can propagate when the pressure inside the electrolyte exceeds the critical value p_{cr}.
- $p_{O_2}^{TPB}$ is the highest pressure can be reached.
- $p_{O_2}^{TPB} > p_{cr}$: crack can propagate

Wang. Y. et al. *Journal of The Electrochemical Society, 2022 169 044529*

Propagation of a Crack

$$\frac{dc}{dt} = \frac{3k}{16\pi\gamma_{eff}c}\left(\mu_{O_2}^{TPB} - \mu_{O_2}^{crack}\right)$$

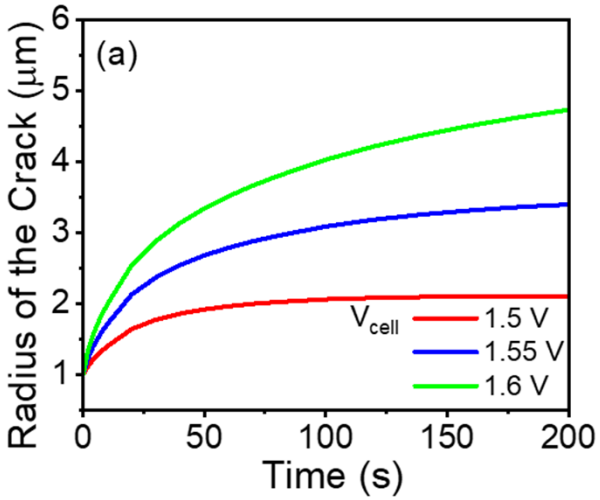

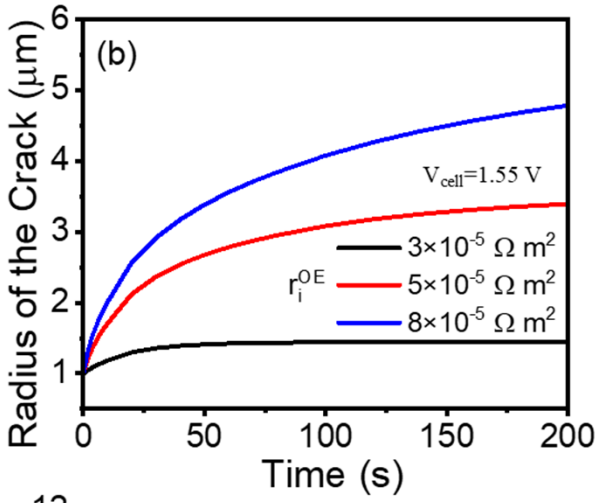

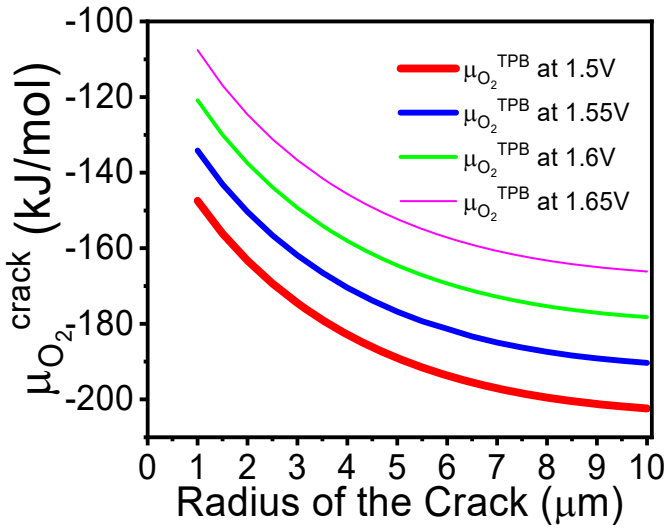

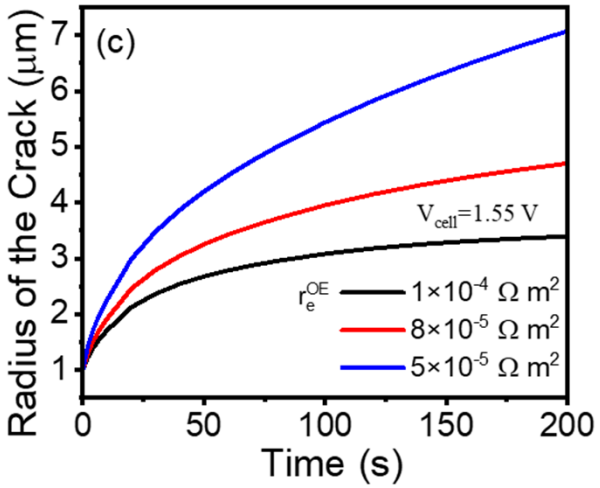

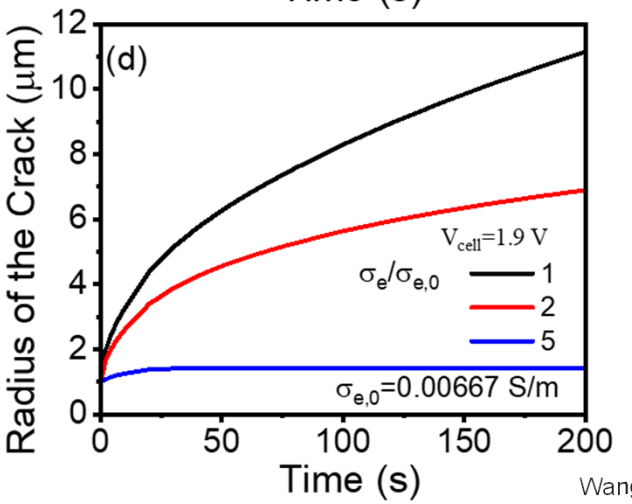

Crack growth ↑

- A higher electrolysis voltage
- A higher r_i^{OE}
- A lower r_e^{OE}
- A higher σ_e

Wang. Y. et al. *Journal of The Electrochemical Society, 2022 169 044529*

High Performance SOEC – Thinner Electrode

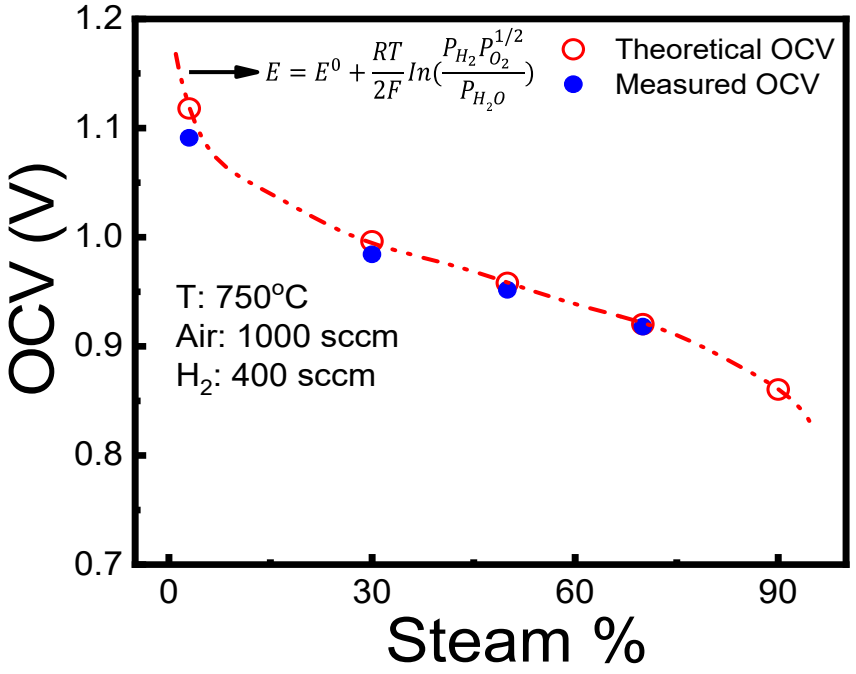

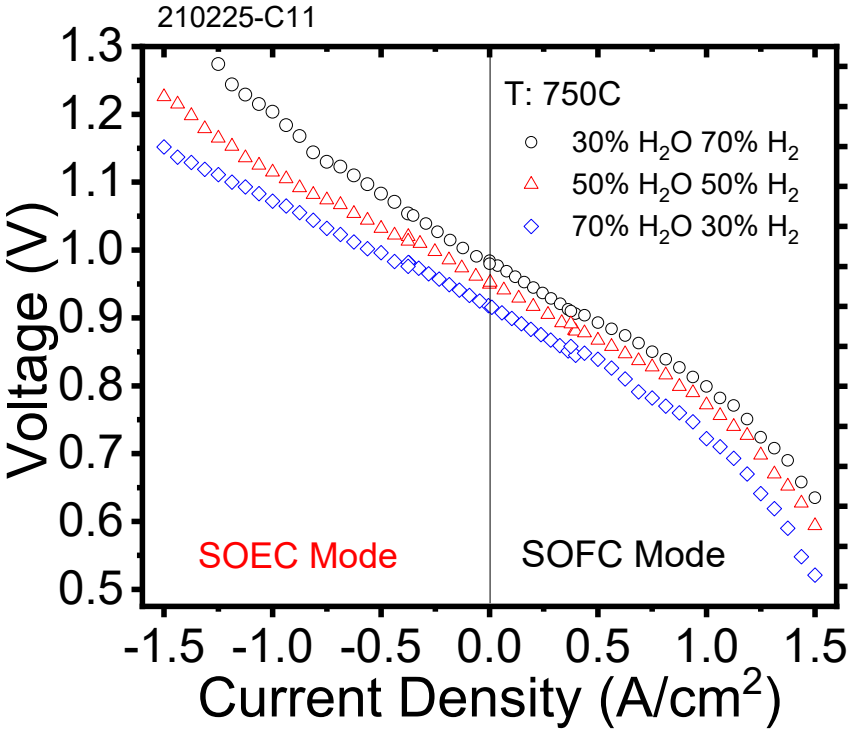

$$\boldsymbol{i} = \left(1 - \frac{L}{L - \frac{\boldsymbol{\varepsilon}}{\boldsymbol{\tau}} \frac{p}{RT} \frac{D_{\alpha,\beta} D_{K,\alpha}}{D_{K,\alpha} + D_{\alpha,\beta}} \frac{z_\alpha F}{i_0}}\right) y_{\alpha 0} i_0$$

Role of Microstructures: the porosity (ε) and tortuosity (τ).

A high ε/τ value will result in a high Faradaic current at the electrolyte/ electrode interface.

Reversible Cell Performance

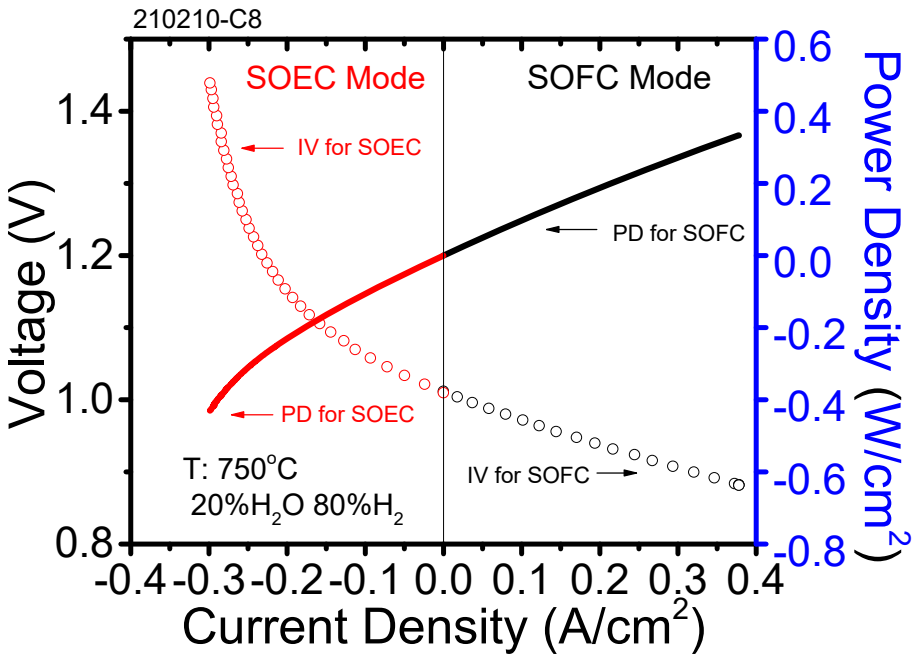

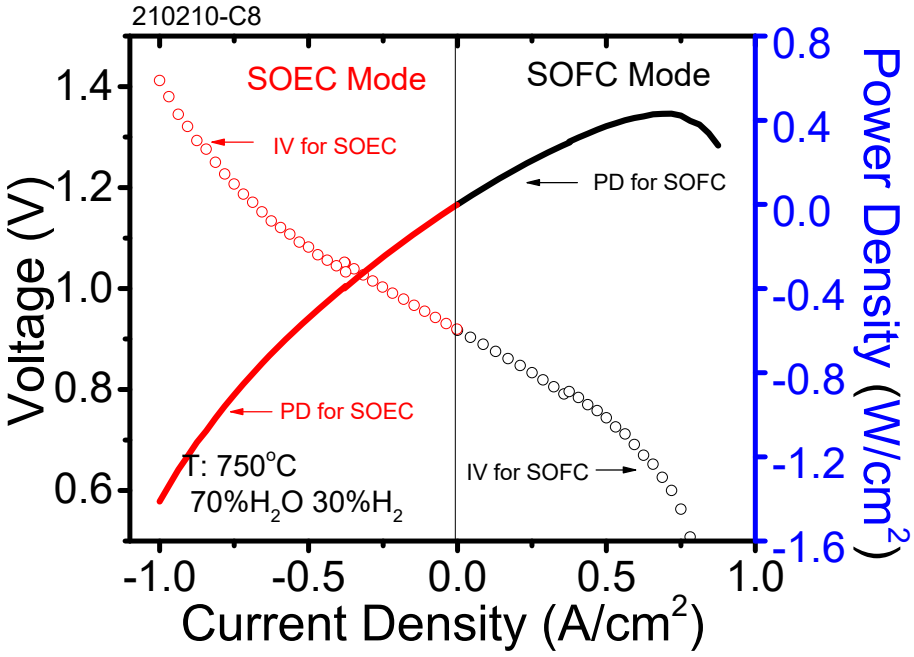

Steam %	OCV theoretical	OCV measured
3	1.118 V	1.087 V
20	1.021 V	1.011V
70	0.920 V	0.917 V

The good match between theoretical OCV and measured OCV indicates good seal and the correct steam concentration.

Effect of Interlayer on SOFC Performance

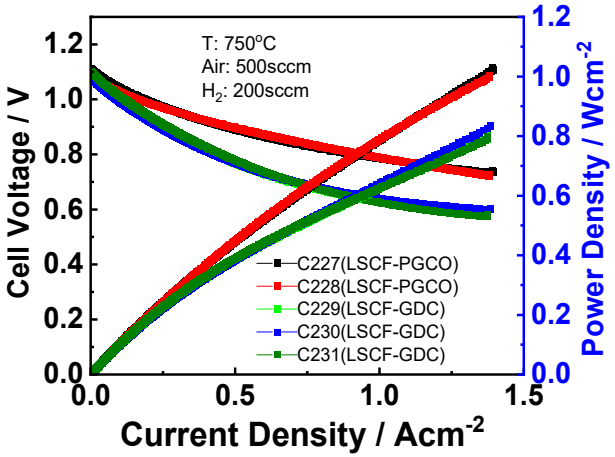

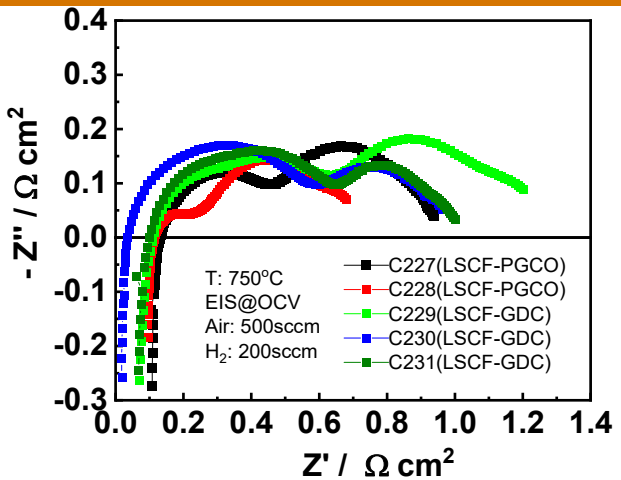

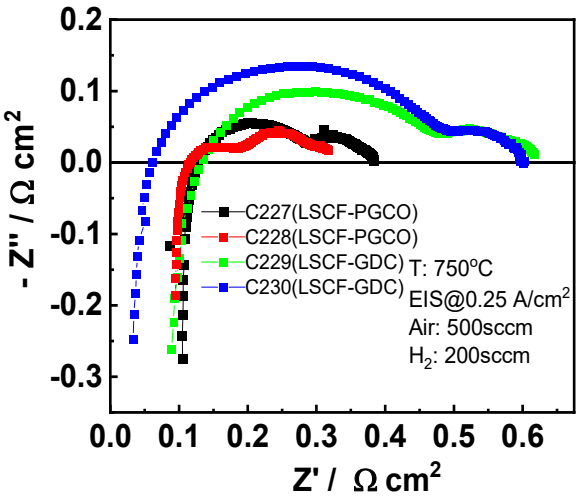

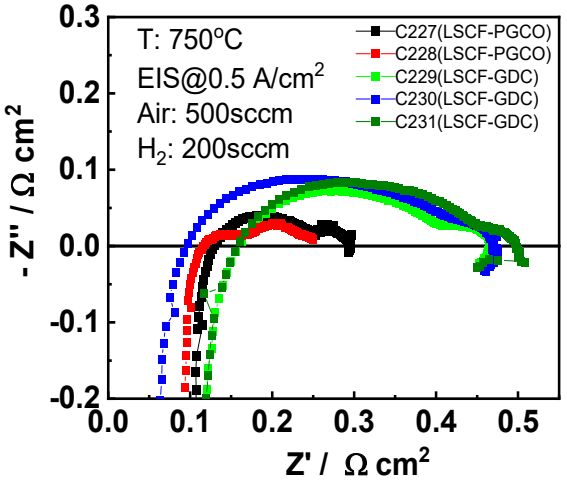

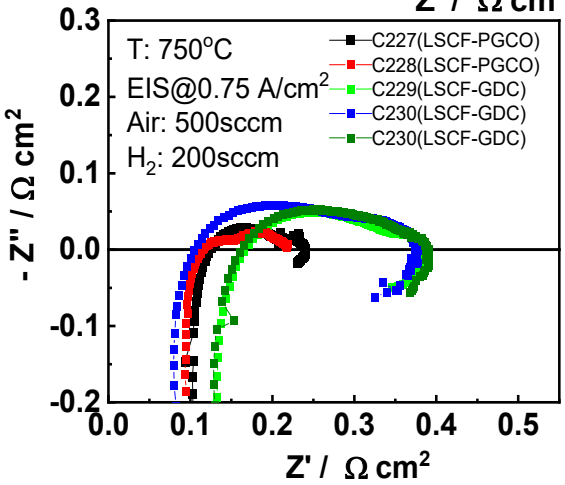

COMPOSITION

- Anode – NiO -YSZ (commercial)
- Cathode – LSCF

❖ Observation

- Polarization resistance is relatively higher in GDC cells as observed before
- Ohmic ASR is observed to change with current density especially in GDC cells

Effect of Interlayer SOEC Performance

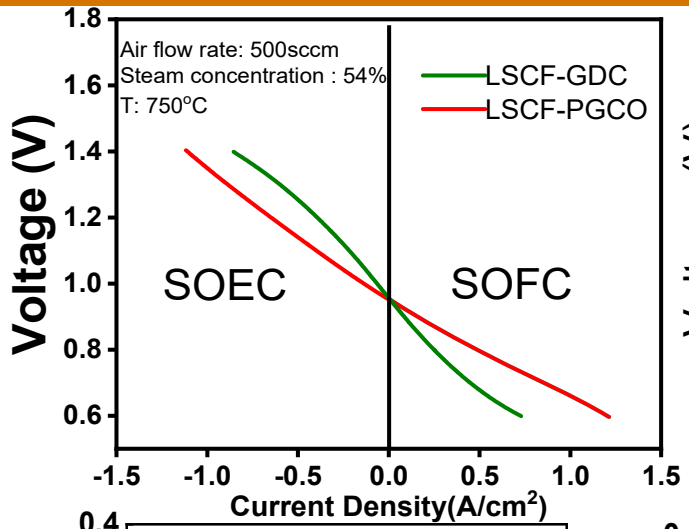

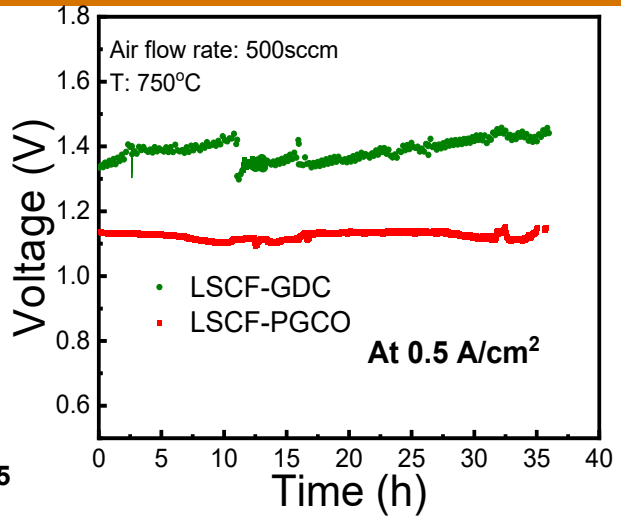

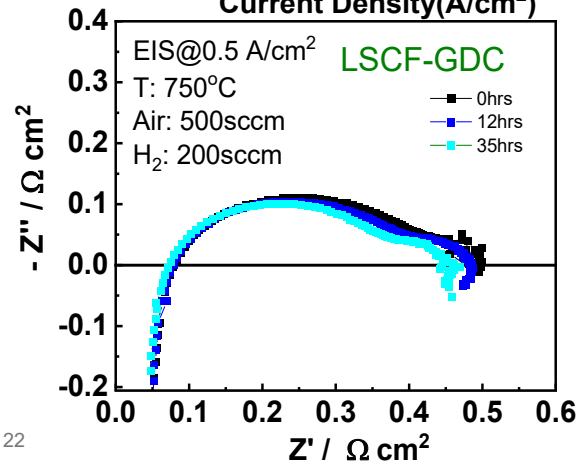

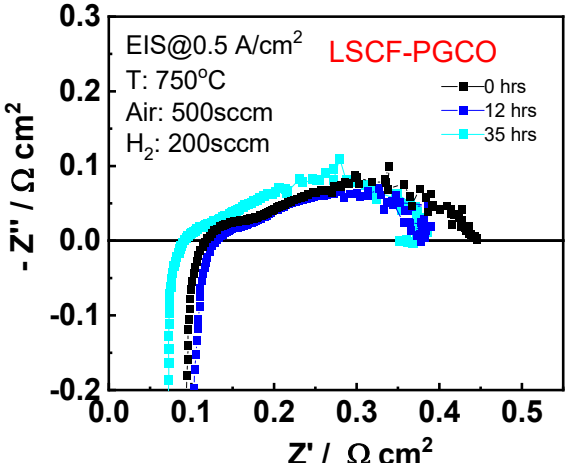

- ❑ **~32% improvement in water splitting current density at 1.4V was achieved with PGCO buffer layer.**
- ❑ **Cathode activity is enhanced by substituting GDC with PGCO**

- ❑ A significant decrease in ohmic ASR is observed in PGCO cell with time as compared to cell with GDC.
- ❑ An increase in initial performance is noticed even after 12hrs of operation for both cells
- ❑ Longer cell durability test time will be needed to compare degradation rates of both cells.

Machine vision processing of microstructural images acquired from electron microscopy

We obtained a set of 326 SEM images (Slice id # from 001 to 651 in increments of 2), each of which is 1536 by 1024, 8 bits per pixel. We initiated work to detect and track the pores in this initial set.

Our goal in this phase is to extract the holes, represented by the black image regions (hereinafter referred to as "blobs"), and track them. We can then calculate the tortuosity measure from the sequence of tracked blobs.

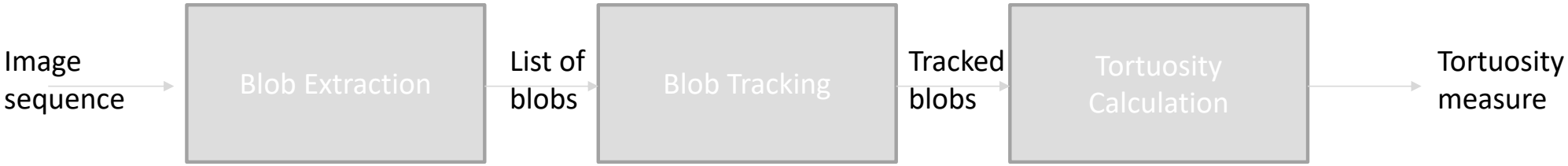

- Segmentation
- Post segmentation clean up

- Tracking based on matching location, shape, size of blobs

- Based on the length of the path that joins the list of tracked blobs

The extraction and tracking processes are being developed in parallel. The ultimate goal is to use deep learning for extraction of the blobs.
To facilitate the development of the tracking process, we temporarily use a simple thresholding method to extract the blobs.

Image SegmentationS

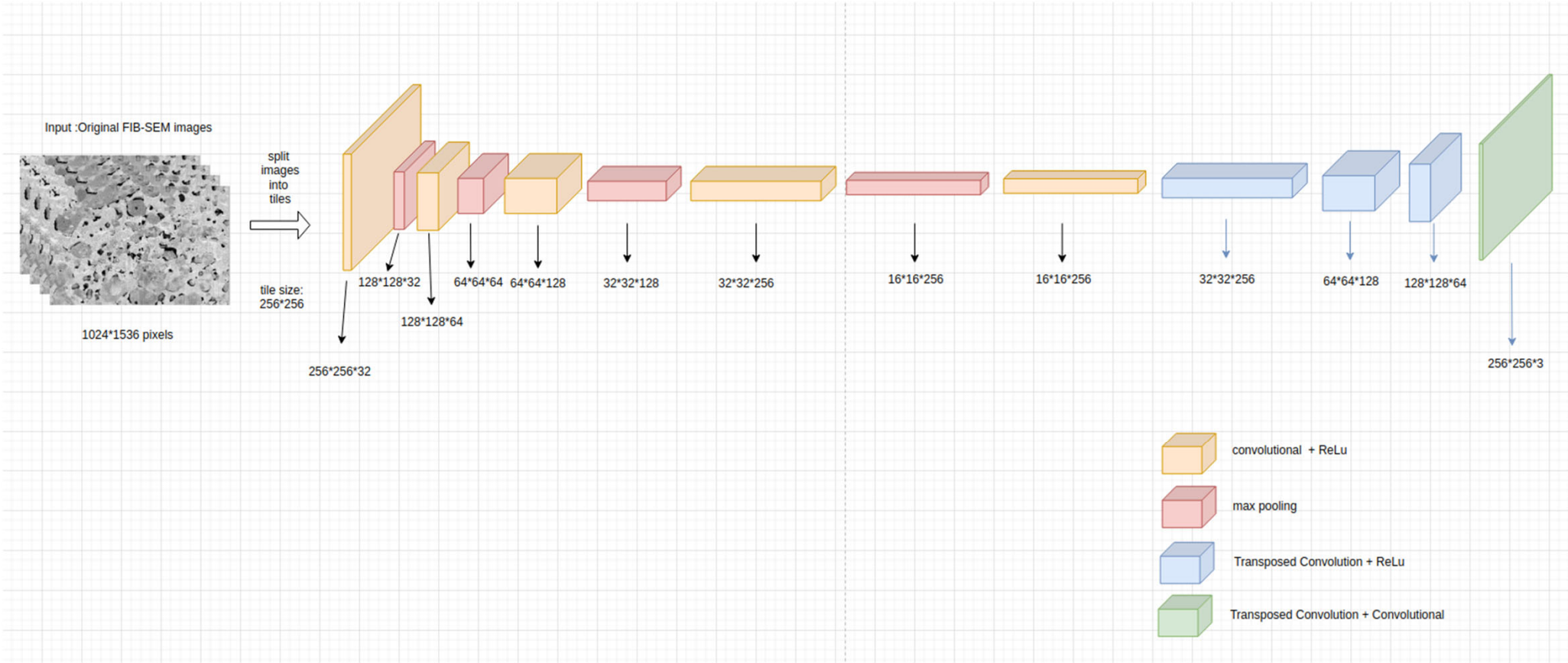

Blob Tracking

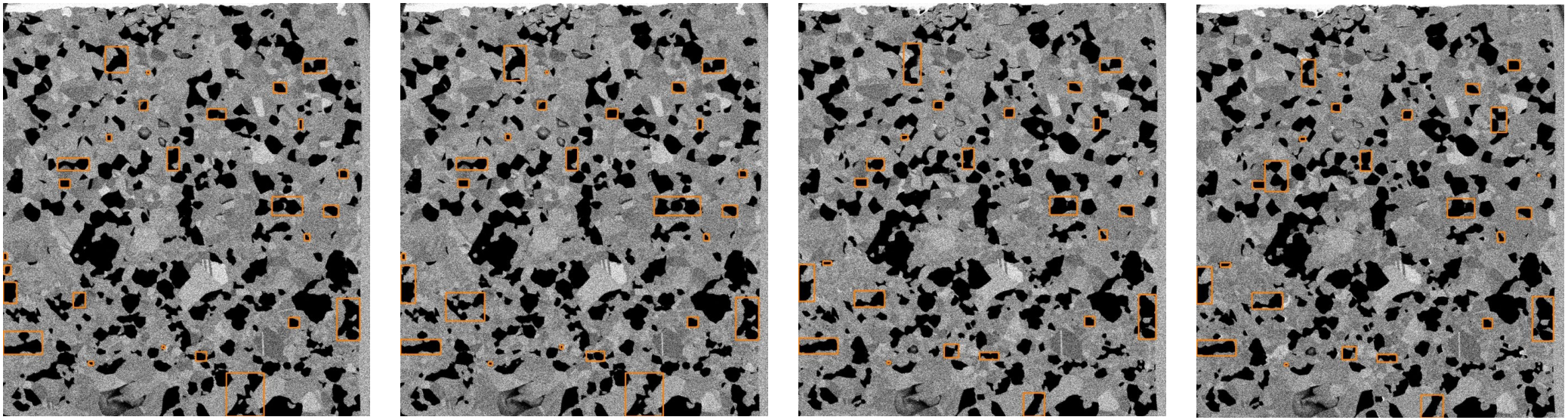

A sequence of 4 slices (Slice ID #323 to 329) shown left to right. A random set of 26 blobs (bounding boxes in orange) were selected from Slice 323 (left) and tracked in the 4 slices using blob location.

Ongoing work is to incorporate shape and size in the matching criterion and to allow forking or joining of tracked paths

Tortuosity

- Suppose we have a sequence of N tracked blobs with centroids $\mathbf{x}_i$ for $i = 0, \cdots, N-1$
- Let d_s be the shortest distance between $\mathbf{x}_0$ and $\mathbf{x}_{N-1}$ so that $d_s = ||\mathbf{x}_0 - \mathbf{x}_{N-1}||$
- Let d_p be the path distance from blob to blob: $d_p = \sum_{i=0}^{N-2} ||\mathbf{x}_i - \mathbf{x}_{i+1}||$
- Define Tortuosity τ as

$$\tau(\{\mathbf{x}_0, \cdots, \mathbf{x}_{N-1}\}) = \frac{d_s}{d_p}$$

- τ varies between 0 and 1
  $\tau = 1$ when $d_p = d_s$ the shortest distance

Development and Understanding of High-Performance Solid Oxide Electrolysis Cells

PI: Xiao-Dong Zhou

Stuller Endowed Chair in Chemical Engineering
Institute for Materials Research and Innovation
University of Louisiana at Lafayette
Lafayette, LA 70503
Email: zhou@louisiana.edu

PM: Evelyn Lopez

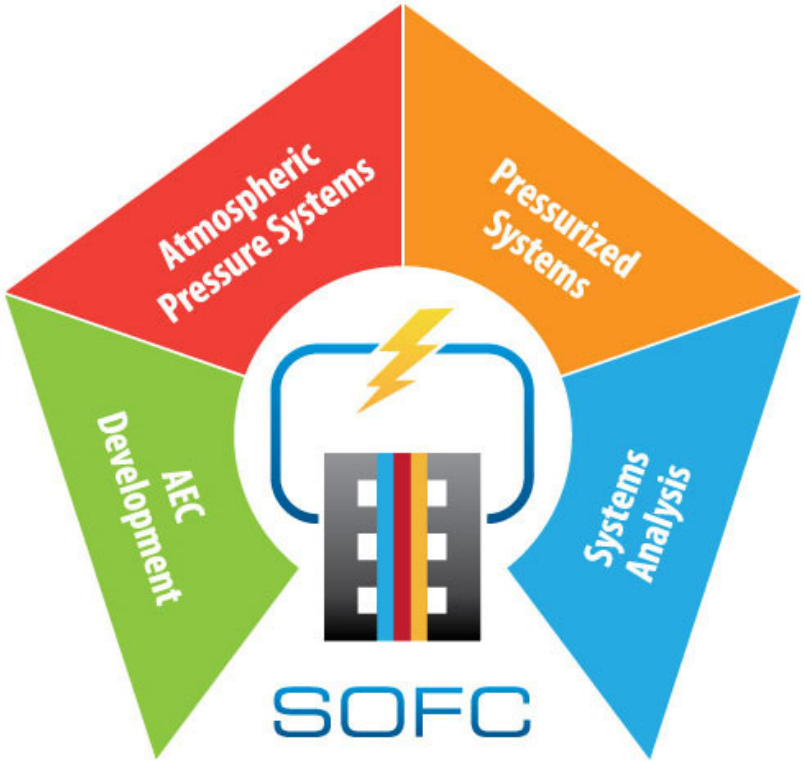

9:30 am on October 27, 2022; DE-FE0032110